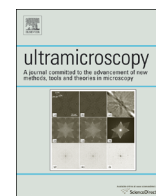




ELSEVIER

Contents lists available at ScienceDirect

## Ultramicroscopy

journal homepage: [www.elsevier.com/locate/ultramic](http://www.elsevier.com/locate/ultramic)

## Annular dark field transmission electron microscopy for protein structure determination

Philip J.B. Koeck

Royal Institute of Technology, School of Technology and Health and Karolinska Institutet, Department of Biosciences and Nutrition, Novum, 14183 Huddinge, Sweden

## ARTICLE INFO

## Article history:

Received 16 April 2015

Received in revised form

27 October 2015

Accepted 21 November 2015

Available online 23 November 2015

## Keywords:

Annular dark field aperture

Weak phase and amplitude object approximation

Phase contrast transfer function

Resolution

Linear imaging

Projection approximation

Transmission electron microscopy

## ABSTRACT

Recently annular dark field (ADF) transmission electron microscopy (TEM) has been advocated as a means of recording images of biological specimens with better signal to noise ratio (SNR) than regular bright field images. I investigate whether and how such images could be used to determine the three-dimensional structure of proteins given that an ADF aperture with a suitable pass-band can be manufactured and used in practice. I develop an approximate theory of ADF-TEM image formation for weak amplitude and phase objects and test this theory using computer simulations. I also test whether these simulated images can be used to calculate a three-dimensional model of the protein using standard software and discuss problems and possible ways to overcome these.

© 2015 Elsevier B.V. All rights reserved.

## 1. Introduction

One of the current frontiers in cryo TEM is the structure determination of relatively small proteins, with a mass below about 300 kDa. One way to reach this goal is to increase the signal to noise ratio (SNR) of the images recorded. ADF-TEM has been recently suggested as one possible imaging mode for achieving this purpose [14]. These ideas, however, date back much further in the history of electron microscopy. The earliest realization of ADF-TEM on inorganic specimens is presented in [9] based on earlier theoretical work referenced therein. Ottensmeyer and co-workers were among the earliest to apply dark field TEM (by tilting the beam) to biological specimens [17] and to attempt the three-dimensional reconstruction of a macromolecule based on dark field TEM micrographs [18,19]. However, these attempts were made before the invention of cryo-preservation of aqueous specimens [4]. Later the high contrast of dark field imaging was also exploited in ADF-STEM in order to determine three-dimensional protein structures [16,3]. The motivation for all these experiments was to exploit the high SNR of dark field imaging to be able to image small proteins with sufficiently high quality for 3D-reconstruction. In contrast to

this, dark field STEM has also been suggested as a means of imaging thick cryo-sections of cells for tomographic reconstruction of cellular structures owing to the higher image quality achievable for thick and highly tilted sections compared to conventional cryo electron tomography.

Obviously high contrast is not the only requirement for being able to use a particular imaging mode in quantitatively correct three-dimensional (3D) structure determination at high resolution. There also has to be a well-defined mathematical relationship between the specimen (in this case the electrostatic potential of a protein) being imaged and the images. Additionally, methods for inverting this relationship have to exist. For example, to be able to use filtered backprojection for 3D reconstruction, the images should, after deconvolution of a known point spread function, be proportional to the projection of the specimen. As a first test whether ADF-TEM imaging could be used for structure determination I have therefore carried out image formation simulations in ADF mode and calculated 3D reconstructions using standard software (EMAN) based on these simulated images. To be able to specify the mathematical relationship between the specimen and ADF-TEM images I also outline an approximate image formation theory valid under certain circumstances. In contrast to the ADF aperture used in [14], which has a quite narrow passband at very high resolution I simulate images for an ADF aperture with a passband between 50 and 5 Å resolution for a  $C_s$  of 2 mm and between 50 and 2.5 Å resolution for a  $C_s$  of 0.1 mm. I make no

*Abbreviations:* TEM, transmission electron microscopy/microscope; STEM, scanning transmission electron microscopy/microscope; ADF, annular dark field; SNR, signal to noise ratio; 3D, three-dimensional; POA, phase object approximation

*E-mail address:* [Philip.Koeck@ki.se](mailto:Philip.Koeck@ki.se)

<http://dx.doi.org/10.1016/j.ultramic.2015.11.010>

0304-3991/© 2015 Elsevier B.V. All rights reserved.

claim whether such an aperture can be manufactured or used, but I investigate whether it would be worth trying.

## 2. ADF-TEM image formation

In order to specify exactly how the simulations presented in the following sections were carried out I list here the main assumptions of the well-established description of image formation for weak and semi-weak amplitude and phase objects. I then make specific modifications and approximations for the case of annular dark field transmission electron microscopy of weak amplitude and phase objects. I also state which particular conventions regarding signs, for example, I follow.

In the phase-object-approximation (POA) the wave exiting the specimen (exit wave) can be written as

$$\psi_{ex}(\mathbf{x}, z, t) = \psi_i(z, t) e^{i\sigma \phi(\mathbf{x})} \quad (1)$$

where  $\psi_i(z, t)$  is the incoming electron wave (a plane wave with wavelength  $\lambda_i$  travelling in  $z$ -direction, with amplitude 1 for simplicity). I use the convention of writing the plane wave as:

$$\psi_i(z, t) = e^{2\pi i(kz - \nu t)} \quad (2)$$

The object  $\phi(\mathbf{x})$ , that is being imaged in the microscope, is the projection of the specimen's electrostatic potential  $V(x, y, z)$  along the optical axis ( $z$ -axis) and

$$\sigma = \frac{2\pi m e \lambda_i}{h^2} \quad (3)$$

is the positive valued interaction constant.

(See e.g. [2,23,24,6,20])

Bold letters are used for vectors in two dimensions in this paper so that for example  $\mathbf{x}$  stands for the coordinates  $(x, y)$  in real space whereas  $\mathbf{u}$  stands for the corresponding Fourier coordinates or two-dimensional wave vector  $(u, v)$ .

Amplitude contrast can be included in this model by letting the potential and therefore the object  $\phi(\mathbf{x})$  be a complex valued function [5,6]. The imaginary part of this complex potential has to be positive in order to describe amplitude reduction.

The exit wave given in Eq. (1) is propagated through the lens system of the electron microscope and finally produces an image on the detector. These processes can be summarized as follows:

A lens produces the Fourier transform of the exit wave in its focal-plane and the effect of the lens aberrations can be described as a multiplication of this Fourier transform with a phase factor containing the lens aberration function in its argument [20].

$$\psi_{pc}(\mathbf{u}, z, t) = FT[\psi_{ex}(\mathbf{x}, z, t)] e^{-i\chi(u)} \quad (4)$$

This modified exit wave is inversely Fourier transformed while it propagates to the image plane where it then produces an image on the detector [8].

An image of the modified exit wave is proportional to the absolute square of the wave-function [20]. Here I have also made it explicit that the image is a function of only  $\mathbf{x}$  since the dependence on  $z$  and  $t$  cancels when the absolute square of the wave function is calculated, as can be seen from Eqs. (1) and (2).

$$i(\mathbf{x}) = |\psi_{pc}(\mathbf{x}, z, t)|^2 \quad (5)$$

The lens aberration function (see for example [20] or [6]) is given by

$$\chi(u) = \pi D \lambda u^2 + \frac{\pi}{2} C_s \lambda^3 u^4 \quad (6)$$

where  $u$  is the spatial frequency, the magnitude of the wave vector

$\mathbf{u}$ ,  $D$  is the defocus ( $D$  is negative for underfocus, positive for overfocus),  $\lambda$  is the wavelength of the electron and  $C_s$  is the spherical aberration coefficient. This form of the lens aberration function is valid in the absence of astigmatism.

Partial spatial coherence is taken into account by multiplying the Fourier transform of the exit wave with a Gaussian envelope.

For finite values of the product  $\sigma\phi(\mathbf{x})$  we can develop Eq. (1) into a McLaurin series which, considering only terms up to the second order for relatively weak amplitude and phase objects, gives

$$\psi_{ex}(\mathbf{x}, z, t) \approx \psi_i(z, t) \left[ 1 + i\sigma \phi(\mathbf{x}) - \frac{\sigma^2}{2} \phi^2(\mathbf{x}) \right] \quad (7)$$

The Fourier transform with respect to  $\mathbf{x}$  of this expression is

$$\psi_{ex}(\mathbf{u}, z, t) \approx \left[ \delta(\mathbf{u}) + i\sigma F(\mathbf{u}) - \frac{\sigma^2}{2} F_d(\mathbf{u}) \right] \psi_i(z, t) \quad (8)$$

where  $F(\mathbf{u})$  is the Fourier transform of  $\phi(\mathbf{x})$  and  $F_d(\mathbf{u})$  is the Fourier transform of  $\phi^2(\mathbf{x})$ :

$$F_d(\mathbf{u}) = FT[\phi^2(\mathbf{x})] = FT[\phi(\mathbf{x})] * FT[\phi(\mathbf{x})] = F(\mathbf{u}) * F(\mathbf{u}) \quad (9)$$

The symbol  $*$  stands for convolution.

The Fourier transform of the exit wave-function (8) is modified by the lens as specified in Eq. (4) ([20] leading to:

$$\begin{aligned} \psi_{pc}(\mathbf{u}, z, t) &= \psi_{ex}(\mathbf{u}, z, t) e^{-i\chi(u)} \\ &\approx \left[ \delta(\mathbf{u}) + i\sigma F(\mathbf{u}) - \frac{\sigma^2}{2} F_d(\mathbf{u}) \right] e^{-i\chi(u)} \psi_i(z, t) \end{aligned} \quad (10)$$

The image can therefore be written as:

$$\begin{aligned} i(\mathbf{x}) &= |\psi_{pc}(\mathbf{x}, z, t)|^2 = \left| \int d\mathbf{u} e^{2\pi i \mathbf{x} \cdot \mathbf{u}} \psi_{pc}(\mathbf{u}, z, t) \right|^2 \\ &\approx \left| \int d\mathbf{u} e^{2\pi i \mathbf{x} \cdot \mathbf{u}} \left[ \delta(\mathbf{u}) + i\sigma F(\mathbf{u}) - \frac{\sigma^2}{2} F_d(\mathbf{u}) \right] e^{-i\chi(u)} \psi_i(z, t) \right|^2 \end{aligned} \quad (11)$$

An ADF aperture removes all spatial frequencies below a given value from the exit wave. Therefore the first term, containing  $\delta(\mathbf{u})$ , in the above equation will not contribute and the lowest order term of the dark field image becomes:

$$i_{df}(\mathbf{x}) \approx \sigma^2 \left| \int d\mathbf{u} e^{2\pi i \mathbf{x} \cdot \mathbf{u}} F(\mathbf{u}) A(u) e^{-i\chi(u)} \right|^2 \quad (12)$$

All terms containing  $\sigma$  taken to the power of 3 and higher are assumed to be much smaller than the term given in Eq. (12) and therefore ignored.

$A(u)$  describes the effect of the ADF aperture as follows:

$$A(u) = \begin{cases} 1 & \text{for } u_{\min} < u < u_{\max} \\ 0 & \text{else} \end{cases} \quad (13)$$

In the above derivations I have made no special assumption about the absorption potential, other than its being real valued. However for the following approximation and the simulations in the next section I will assume that the absorption potential is a small, fixed percentage of the real potential (7%). This is a commonly used assumption for specimens consisting of mainly one type of atom ([7]).

When recording an image close to focus the lens aberration function is approximately zero for the lowest spatial frequencies up to about 5 Å resolution in the case of a spherical aberration of 2 mm and a defocus of 13 nm as shown by the plot labelled “ $C_s = 2$  mm” in Fig. 1. For lower values of the  $C_s$  this resolution range can be extended, for example to better than 2.5 Å in the case of a  $C_s$  of 0.1 mm and a defocus of 3 nm, shown by the plot labelled “ $C_s$

Download English Version:

<https://daneshyari.com/en/article/8037972>

Download Persian Version:

<https://daneshyari.com/article/8037972>

[Daneshyari.com](https://daneshyari.com)